

# A comparison between cylindrical and cross-shaped magnetic vibration isolators: ideal and practical

D.T.E.H. VAN CASTEREN, J.J.H. PAULIDES, E.A. LOMONOVA

*Eindhoven University of Technology  
Electromechanics and Power Electronics group  
Den Dolech 2, 5600MB Eindhoven, The Netherlands  
e-mail: d.t.e.h.v.casteren@tue.nl*

(Received: 10.09.2015, revised: 20.09.2015)

**Abstract:** In this paper a cross-shaped isolator consisting of cuboidal magnets and a cylindrical isolator are compared by resonance frequency to volume ratio and shape. Both isolators are capable of obtaining a low resonance frequency, i.e. 0.15 Hz and 0.01 Hz for the cross and cylinder, respectively. The volume of both isolators is comparable, only the shape is different, resulting in a tall structure with a small footprint for the cross and a flat with a large diameter cylindrical structure. A sensitivity analysis shows that due to the large amount of magnets, the cross-shaped isolator is less sensitive to manufacturing tolerances.

**Key words:** Gravity compensation, magnetic, vibration isolation.

## 1. Introduction

For precision machines the influence of floor vibrations and acoustic disturbances become ever more critical. In these high-precision systems, therefore, the demands on vibration isolation systems increase. Currently, the most mature technique for vibration isolation is air bearings augmented by linear actuators. These air bearings can, however, not work in a vacuum, which is required for an extreme ultraviolet lithography system, for instance. To cope with the requirements, research is dedicated to magnetic vibration isolation systems which have the advantages of being contactless. Therefore, no lubricants are required, making it vacuum compatible.

A magnetic vibration isolation system consists of a magnetic spring (gravity compensator) which generates a vertical force to levitate the mass, while maintaining a low stiffness to isolate the mass from floor vibrations. Since a magnetic spring is always unstable, linear actuators are present to stabilize the system.

Magnetic vibration isolators can come in many shapes, such as cylindrical [1], conical [2], planar (vertical and horizontal) [3], etc. In this paper a comparison is made between two practical isolators. The first isolator which is discussed consists of cuboidal magnets placed in a cross [4], which can be seen in Figure 1(a). The second isolator uses cylindrical magnets [5].

The translator consists of two axially magnetized magnets and the stator magnet is magnetized radially, as can be seen in Figure 1(b).

An important characteristic is the resonance or isolation frequency. This determines from which frequency the isolator starts to reduce the vibrations from the floor. In general, this frequency is desired to be as small as possible in order to reduce as much vibration as possible. Since the volume of the isolator is also important, in this paper, two isolator types are compared by volume and resonance frequency [6].

Another important characteristic is the manufacturability of these isolators. The calculations assume identical magnets, this is, however, not the case in reality and small deviations on size and magnetization are always present. As in [7] the influences of these deviations are shown by means of a sensitivity analysis.

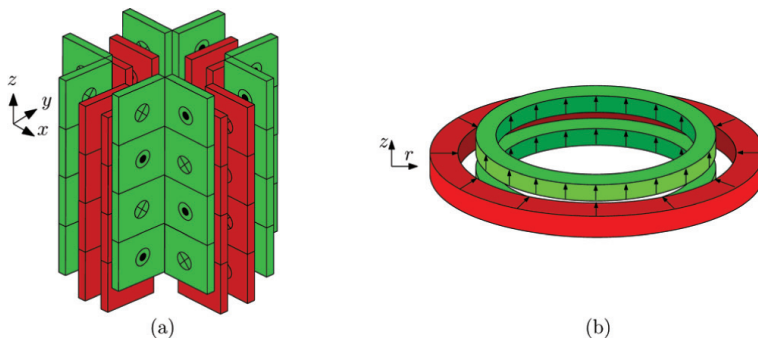


Fig. 1. Magnetic structure of the (a) cross-shaped, and (b) cylindrical isolator

To compare these isolators, first the calculation of force, stiffness, and resonance frequency of a gravity compensator is explained. Second, the comparison is made for a fixed vertical force. Third, the optimal designs are subjected to a sensitivity analysis. Finally, conclusions are made.

## 2. Characteristic calculation

A gravity compensator has four important characteristics, namely vertical output force, stiffness, resonance frequency, and volume. To calculate these characteristics, first the magnetic flux density is calculated. Since the gravity compensators are in free space and only consist of permanent magnets, the charge model is ideal (under the assumption that the relative permeability is unity).

If the magnetization vector  $\vec{M}$  is confined to the magnet volume  $V$  with surface  $S$ , and falls abruptly to zero outside this volume, the magnetic field,  $\vec{B}$ , is calculated using

$$\vec{B} = \frac{\mu_0}{4\pi} \left[ \iiint_V \rho \frac{\vec{r} - \vec{r}'}{|\vec{r} - \vec{r}'|^3} dV' + \iint_S \sigma \frac{\vec{r} - \vec{r}'}{|\vec{r} - \vec{r}'|^3} dS' \right], \quad (1.1)$$

where  $r$  and  $r'$  are the observation and source point, respectively [8]. The volume and surface charge density,  $\rho$  and  $\sigma$ , respectively, are calculated by

$$\rho = \nabla \cdot \vec{M}, \quad (1.2)$$

$$\sigma = \vec{M} \cdot \vec{n}, \quad (1.3)$$

where  $\vec{M}$  is the magnetization vector. Note that it is assumed that the relative permeability,  $\mu_r$ , of the magnets is unity. In case of low values of  $\mu_r$  (1,...,1.1) the magnets can be modeled by scaling the charge density with [9].

$$\frac{2}{\mu_r + 1}$$

The force between 2 magnets is calculated using the Lorentz force equation. The force on magnet 1,  $\vec{F}_1$ , is calculated by

$$\vec{F}_1 = \iiint_V \rho_1 \vec{B}_2 dV' + \iint_S \sigma_1 \vec{B}_2 dS', \quad (1.4)$$

where  $\rho_1$  and  $\sigma_1$  are the volume and surface charge density of magnet 1, respectively, and  $\vec{B}_2$  is the magnetic flux density generated by magnet 2. The stiffness,  $\mathbf{K}$ , can be calculated directly from the force equation by

$$\mathbf{K} = -\mathbf{J}(\vec{F}), \quad (1.5)$$

where  $\mathbf{J}$  is the Jacobian. Using the vertical force,  $F_z$ , and stiffness matrix,  $\mathbf{K}$ , the resonance frequency matrix,  $\mathbf{f}_r$ , of the vibration isolator is calculated by

$$\mathbf{f}_r = \frac{1}{2\pi} \sqrt{\frac{\mathbf{K} \mathbf{g}}{F_z}}, \quad (1.6)$$

where the gravitation constant is denoted by  $g$ . Note that negative stiffness results in a virtual, imaginary resonance frequency. In the results this is denoted as a negative resonance frequency.

In the case of cuboidal magnets with homogeneous magnetization, there is only a surface charge density and the force can be solved with analytical equations [10]. This results in an analytical expression for the stiffness and resonance frequency.

For cylindrical magnets this is not the case. The axial magnetized cylinder also consists of surface charges, but the radial magnet also consists of volume charges [11]. The field, however, can only be calculated semi-analytically. Therefore, the force, stiffness, and resonance frequency are calculated numerically.

To estimate the volume of the isolators the smallest possible cube and cylinder is used in which the cross-shaped and cylindrical isolator, respectively, fit.

### 3. Comparison

To attempt a fair comparison between the two structures, several design parameters are fixed. First of all, the airgap,  $l_g$ , between the translator and stator magnets is set to 4 mm, and the scaled remanent magnetization is 1.28 T. Furthermore, the vertical output force of the isolator should be around 3 kN.

#### 3.1. Parameter variation

In Figure 2 the side views of the isolators are given. For the cross-shaped isolator, Figure 2a, the magnets on both the translator and stator are chosen to have equal width  $w_m$ , height,  $h_m$ , and depth,  $d_m$ . The distance between the stator magnets is given by  $w_i$  and the offset of the translator is denoted by  $h_{off}$ . The range in which these parameters are varied are listed in Table 1.

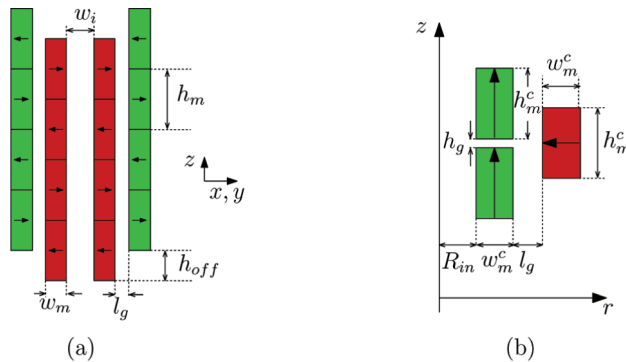


Fig. 2: Cross-section of the (a) cross-shaped, and (b) cylindrical isolator

In Figure 2b the cross-section of the cylindrical isolator is given. As with the cross-shaped isolator, the height,  $h_m^c$ , and width,  $w_m^c$ , of both the stator and translator magnet are chosen equal. The other parameters which are varied, are the inner radius,  $R_{in}$ , and the gap between the translator magnets,  $h_g$ . The range of these parameters are also listed in Table 1.

Table 1. The variation in parameters for the comparison

Cross-shaped		Cylindrical	
Parameter	Range	Parameter	Range
$w_m$	6...12 mm	$w_m^c$	5...110 mm
$w_i$	0...15 mm	$R_{in}$	5...90 mm
$d_m$	10...50 mm	$h_g$	1.5...6 mm
$h_m$	20...50 mm	$h_m^c$	10...50 mm

#### 3.2. Cross-shaped isolator

To obtain a force output of 3 kN, first the force was calculated for a large amount of parameter combinations. In the case of the cross-shaped isolator the parameters,  $w_m$ ,  $w_i$ ,  $d_m$ ,  $h_m$ , are

modeled by 4, 4, 21, 16 steps, respectively. Initially  $h_{off}$  was chosen to be  $1/2 h_m$ . In Figure 3 the calculated force is shown for various values of  $d_m$  and  $h_m$ , while  $w_m$  and  $w_i$  are fixed at 6 mm and 5 mm, respectively.

Since the parameter sweep has coarse steps, to obtain the correct output force, it was chosen to fit the curve using a polynomial approximation. In this case, the parameter  $h_m$  is fixed and the polynomial is used to approximate the force for a much smaller step in  $d_m$ . This leads to the black dots shown in Figure 3.

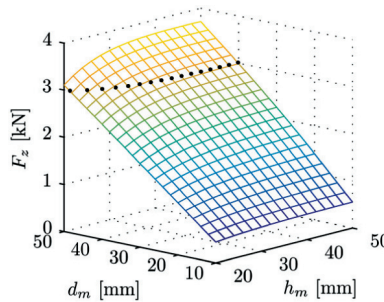


Fig. 3. Force of different combinations when  $w_m = 6$  mm and  $w_i = 5$  mm of the cross-shaped isolator

It can be seen that for the small values of  $h_m$  an increase in  $h_m$  significantly decreases the  $d_m$  required to obtain an output force of 3 kN. For larger values ( $>40$  mm), an increase in height does not alter the force level.

In Figure 4 the difference in force compared to the 3 kN goal is shown for various values of  $h_m$  and different movements. It can be seen that a large force variation occurs for small values of  $h_m$ . Note that to obtain this result the offset of the cross-shaped isolator was not kept equal, but shifted slightly to obtain a symmetric curve.

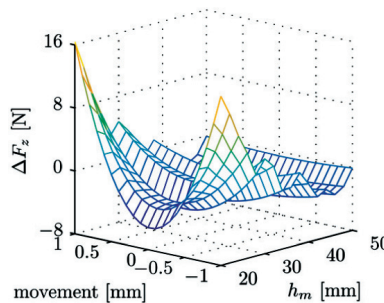


Fig. 4. Force of optimal combination for various movements of the cross-shaped isolator

This symmetry can also be seen in the results of the stiffness and the resonance frequency, Fig. 5a and Fig. 5b, respectively. Here it can also be seen that the large force variation for small  $h_m$ , results in a large stiffness and resonance frequency. These values decrease when the height of the magnets increases.

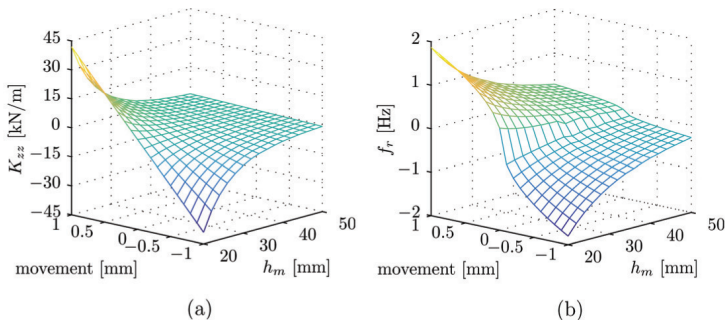


Fig. 5. (a) Stiffness and (b) resonance frequency of optimal combination for various movements of the cross-shaped isolator

The results of the other set of combinations are shown in Fig. 6, where the mean of the absolute resonance frequency is plotted in combination with the volume of the total system. It shows that while increasing the height of the magnets reduces the resonance frequency, it does increase the volume of the isolator. Furthermore, it can be seen that increasing the inner thickness,  $w_i$ , results in a large volume, but not in a decrease in resonance frequency. In this case the optimal width of the magnets is around 8 mm. These lines can, therefore, be used as the optimal region for each  $w_i$ .

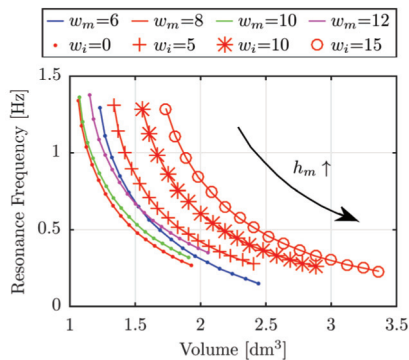


Fig. 6. Volume to resonance frequency plot of the cross-shaped isolator

### 3.3. Cylindrical isolator

For the cylindrical isolator the same steps were taken as with the cross-shaped isolator to obtain a force of 3 kN. The parameters paired in this case were  $R_{in}$  and  $w_m^c$ . An increase in  $R_{in}$  resulted in a decrease in  $w_m^c$ . Using these pairs, the resonance frequency is calculated for the other two parameters,  $h_g$  and  $h_m^c$ . In Figure 7 and Figure 8 the mean resonance frequency versus the occupied volume is shown, when movements of  $-1$  mm till  $0$  mm are taken into account. Due to the symmetry the absolute value is equal to the case when  $-1$  mm to  $+1$  mm is chosen. However, now also a difference in the sign of the steepness is visible, hence the positive and negative resonance frequencies.

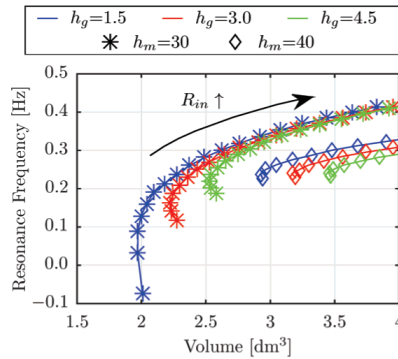


Fig. 7. Volume to resonance frequency plot of the cylindrical isolator for  $h_m^c = 30$  mm and 40 mm

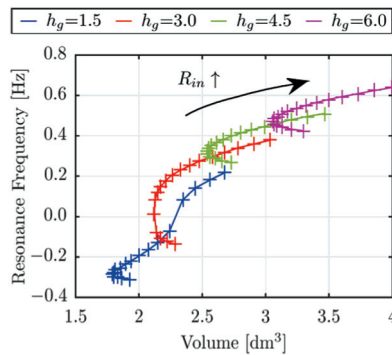


Fig. 8. Volume to resonance frequency plot of the cylindrical isolator for  $h_m^c = 20$  mm

For the cross-shaped isolator the results of the various parameters in one single figure. For the cylindrical structure, this is not possible, since the shape varies more. Therefore, the results have been divided into two figures. In Fig. 7 the results are shown of magnets with  $h_m^c$  is 30 mm and 40 mm for 3 different gaps,  $h_g$  is 1.5 mm, 3.0 mm, and 4.5 mm, respectively. The 6.0 mm gap is omitted, since it is in the same trend and otherwise would make the figure unreadable. The same holds for  $h_m^c = 50$  mm.

For  $h_m^c = 20$  mm the results are different and they are shown in Figure 9. It can be seen that the lines of the different gaps now cross each other. For both figures it can, however, be seen that for each combination there is an optimum volume.

### 3.4. Differences

Looking at the two different structures, it can be seen that the shape of the volume, differ greatly for the two structures. For the cross-shaped structure a larger height is better for low resonance frequencies. The cylindrical isolator, on the other hand, is mainly flat and has a large surface area,  $S$ . To show the difference between the two isolator types the “optimal” isolators

are chosen. In order to obtain an “optimal” isolator, a trade-off is made between the resonance frequency and the volume. In the case of the cross-shaped isolator, the topology is chosen which has,  $w_i = 0$  mm,  $w_i = 8$  mm,  $h_m = 38$  mm,  $d_m = 26$  mm as parameters. The optimal cylindrical structure has  $h_g = 1.5$  mm,  $h_m = 30$  mm,  $R_m = 10$  mm,  $d_m = 43.5$  mm as parameters. In Table 2 the results are shown for the two isolators. It also shows that the volume of the magnets,  $V_{mag}$  is significantly smaller for the cross-shaped structure.

Table 2. Summary of the optimal results

Isolator	$f_r$ [Hz]	$V$ [dm <sup>3</sup> ]	$S$ [dm <sup>2</sup> ]	$V_{mag}$ [dm <sup>3</sup> ]
Cross	0.48	1.5	0.89	0.51
Cylindrical	0.03	2.0	3.9	0.91

## 4. Sensitivity analysis

In the previous section, the optimal sizes of the isolators were determined using a parametric search. In reality, however, it is not possible to exactly match these values due to manufacturing tolerances. To see how sensitive each topology is for manufacturing tolerances, a sensitivity analysis is conducted. For this analysis a 1000 different combinations are modeled, which all are within the tolerance specification. First, the impact of tolerance on the dimension of the magnet is analyzed and second, the influence of magnetization variations of the magnet is analyzed. In order to obtain appropriate results, the vertical offset of the topology is chosen per structure. The zero-position is chosen with consideration for minimizing the resonance frequency.

### 4.1. Magnet dimension

When manufacturing magnets, there are always tolerances on the dimensions of the magnets. A standard value is 0.1 mm. Lower tolerances are possible, however, this comes at the cost of extra expenses.

For the cross-shaped topology, this means that the dimensions of the magnet can become  $w_m = 8 \pm 0.1$  mm,  $h_m = 38 \pm 0.1$  mm, and  $d_m = 26 \pm 0.1$  mm. In Fig. 9 the result is shown of the sensitivity analysis. It can be seen that the vertical force varies ( $\pm 1\%$ ) between the different structures. The resonance frequency also varies about 1%. This is due to the large amount of magnets, which averages the error. Resulting in a small deviation compared to the ideal case.

For the cylindrical topology, the dimensions of the magnets are  $h_g = 1.5 \pm 0.1$  mm,  $h_m = 1.5 \pm 0.1$  mm,  $R_m = 10 \pm 0.1$  mm,  $d_m = 43.5 \pm 0.1$  mm. The result of the sensitivity analysis is shown in Figure 10. Since the variation in size is relatively small, the variation in force is equal to the cross-shaped topology. Due to the small amount of magnets, i.e. 3 magnets, the resonance frequency is more sensitive to size variations, resulting in larger variations ( $\pm 0.2$  Hz).

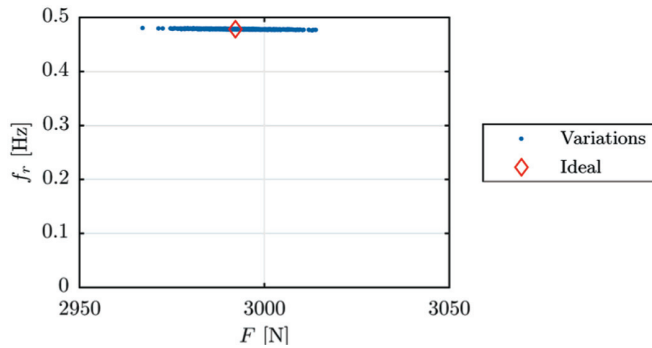


Fig. 9. The resonance frequency versus vertical force for 1000 different possible cross-shaped topologies which satisfy the tolerance on the dimension of the magnets.

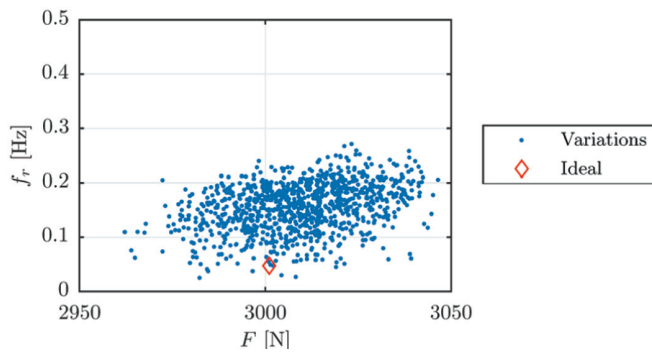


Fig. 10. The resonance frequency versus vertical force for 1000 different possible cylindrical topologies which satisfy the tolerance on the dimension of the magnets.

#### 4.2. Magnetization

Besides the dimensions of the magnets, the magnetization of the magnet is also subjected to tolerances on i.e. magnitude and direction. In this paper, it is assumed that the direction is ideal and the remanent magnetization has a typical value of 1.32 T and a minimal value of 1.28 T. The relative permeability is considered 1.03.

In Figure 11 and Figure 12 the results of the sensitivity analysis are shown for the cross-shaped and cylindrical topology, respectively. Once more, it can be seen that the cross-shaped structure has a small variation in resonance frequency ( $< 0.3\%$ ). It illustrates, however, that the variations do not reach the force obtained with the typical magnetizations. This is due to the large amount of magnets, i.e. 64 in total. Since the magnetization is randomly distributed between 1.28 T and 1.32 T, the average magnetization is equal to approximately the ideal case for each variation and the results are, therefore, centered around this point. It is, however, possible to be in between the typical and minimal case.

The cylindrical structure has more variation in resonance frequency ( $+0.2$  Hz) and the output force covers the entire range from minimal to typical. This is again due to the small amount of magnets.

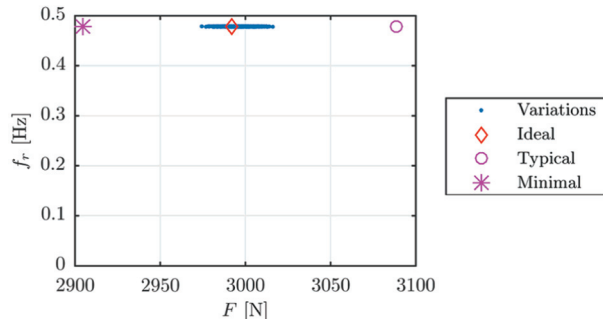


Fig. 11. The resonance frequency versus vertical force for 1000 different possible cross-shaped topologies which satisfy the tolerance on the magnitude of the remanent magnetization of the magnets

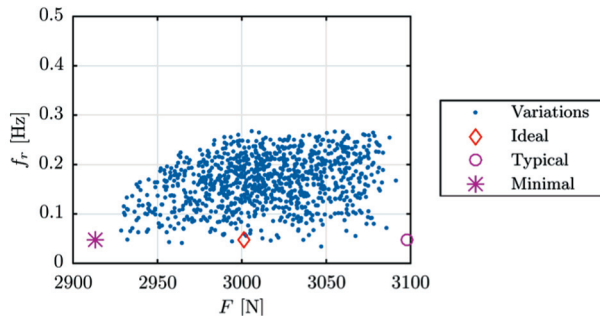


Fig. 12. The resonance frequency versus vertical force for 1000 different possible cross-shaped topologies which satisfy the tolerance on the magnitude of the remanent magnetization of the magnets

Up till now, the cylindrical structure was modeled using an ideal radially magnetized outer magnet. In practice, however, this magnet is usually created by combining multiple smaller magnets with a parallel magnetization, as can be seen in Figure 13. Increasing the amount of magnets increases the resemblance with the radially magnetized magnet as can be seen in Figure 14, which shows the results of 2 to 20 magnets. It can be seen that using parallel magnets only influences the vertical output force, where the resonance frequency does not change. This is due to the magnetic field created by the inner magnets being very constant in the vertical direction, such that movements in the vertical directions do not result in large force variations. Hence a low resonance frequency is obtained.

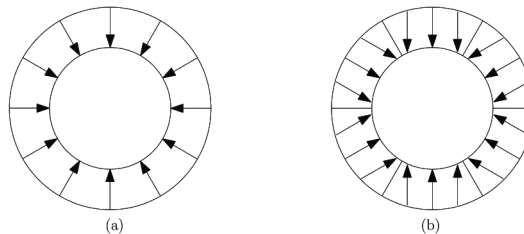


Fig. 13. Radially magnetized cylindrical magnets, (a) ideal and (b) practical

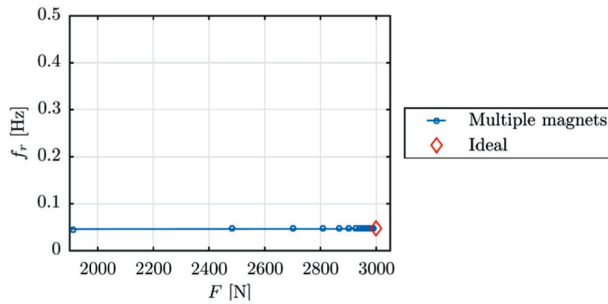


Fig. 14. The resonance frequency versus vertical force when the radial magnet is replaced by multiple parallel magnets

## 5. Conclusions

In this paper two types of vibration isolators are compared, namely a cross-shaped and a cylindrical structure. These are compared by volume and resonance frequency. The results have shown that both structures are able to obtain a very low resonance frequency,  $< 0.2$  Hz. At these values the cross-shaped isolator has a volume of  $2.4 \text{ dm}^3$  and the cylinder  $2.1 \text{ dm}^3$ . The main difference, however, is the shape of the volume. In the case of the cross, a small ground surface is combined with a large height. For the cylinder, this is the opposite, as it has a large ground surface and a small height.

So in most cases the available room in the system will determine the best solution for the vibration isolation application. If there is, however, plenty of room, other factors could be manufacturability and costs.

On the dimensions of the magnets, tolerances are always present. In this paper it was chosen to do a sensitivity analysis for a  $0.1 \text{ mm}$  tolerance on its sizes. Due to the large amount of magnets in the cross-shaped topology, i.e. 64 in total, the global variation in output force and resonance frequency is small,  $< 1\%$  and  $< 0.004 \text{ Hz}$ , respectively. The cylindrical structure uses only 3 magnets, resulting in larger deviations in resonance frequency of about  $0.2 \text{ Hz}$ .

The same can be seen when the influence of variations of the remanent magnetization is verified. For both analyses, however, the absolute value of the resonance frequency is still lower than the cross-shaped topology.

Furthermore, the amount of magnetic material in the cylindrical structure is much larger, which means its costs are higher compared to the cross-shaped structure. If this is important, the cross-shaped isolator is the best topology.

## References

- [1] Deng R., Saathof R., Spronck J.W. et al., *Integrated 6-dof lorentz actuator with gravity compensator for precision positioning*. the 22nd International Conference on Magnetically Levitated Systems and Linear Drives, Rio de Janeiro (2014).
- [2] van Casteren D.T.E.H., Paulides J.J.H., Janssen J.L.G., Lomonova E.A., *Analytical force, stiffness, and resonance frequency calculations of a magnetic vibration isolator for a micro balance*. IEEE Transactions on Industry Applications 51(1): 204-210 (2015).

- [3] Janssen J.L.G., Paulides J.J.H., Lomonova E.A., *Study of Magnetic Gravity Compensator Topologies Using an Abstraction in the Analytical Interaction Equations*. Progress In Electromagnetics Research 128: 75-90 (2012).
- [4] Janssen J.L.G., Gysen B.L.J., Paulides J.J.H., Lomonova E.A., *Advanced Electromagnetic Modeling applied to Anti-Vibration Systems for High Precision and Automotive Applications*. International Compumag Society Newsletter 19(1): 3-16 (2012).
- [5] de Weerdt R.E.M.L., Dams J.A.A.T., *Magnetic actuator under piezoelectric control* European Patent, EP-1424767A2 (2004).
- [6] van Casteren D.T.E.H., Paulides J.J.H., Lomonova E.A., *Gravity Compensation with Cylindrical or Cross-Shaped Magnetic Vibration Isolators*. Proceedings of the 10th International Symposium on Linear Drives for Industry Applications, Aachen, pp 1-4 (2015).
- [7] van Casteren D.T.E.H., Pluk K.J.W., Paulides J.J.H., Lomonova E.A., *Modeling the effects of magnetization variations on a permanent magnet based levitation or vibration isolation system*. Applied Mechanics and Materials 416-417: 366-372. (2013).
- [8] Furlani, E.P., *Permanent Magnet and Electromechanical Devices: Materials, Analysis, and Applications*. Academic press (2001).
- [9] van Casteren D.T.E.H., Paulides J.J.H., Lomonova E.A., *3-D Numerical Surface Charge Model including Relative Permeability: the General Theory*. IEEE Transactions on Magnetics, 50(11): 8204704 (2014).
- [10] Allag H., Yonnet J.P., Latreche M.E.H., *3D Analytical Calculation of Forces between Linear Halbach-Type Permanent-Magnet Arrays*, Advanced Electromechanical Motion Systems & Electric Drives Joint Symposium, Lille, pp. 1-6 (2009).
- [11] Ravaut R., Lemarquand G., Lemarquand V., Depollier C., *Permanent magnet couplings: Field and torque three-dimensional expressions based on the coulombian model*, IEEE Transactions on Magnetics, 45(4): 1950-1958 (2009).